

Towards Principled Design of Mixture-of-Experts Language Models under Memory and Inference Constraints

Seng Pei Liew and Kenta Shinzato and Yuyang Dong

SB Intuitions, Tokyo, Japan

Abstract

Modern Mixture-of-Experts (MoE) language models are designed based on total parameters (memory footprint) and active parameters (inference cost). However, we find these two factors alone are insufficient to describe an optimal architecture. Through a systematic study, we demonstrate that MoE performance is primarily determined by total parameters (N_{total}) and expert sparsity ($s := n_{exp}/n_{topk}$). Moreover, n_{exp} and n_{topk} do not "cancel out" within the sparsity ratio; instead, a larger total number of experts slightly penalizes performance by forcing a reduction in core model dimensions (depth and width) to meet memory constraints. This motivates a simple principle for MoE design which maximizes N_{total} while minimizing s (maximizing n_{topk}) and n_{exp} under the given constraints. Our findings provide a robust framework for resolving architectural ambiguity and guiding MoE design.

1 Introduction

Many publicly available Mixture-of-Experts (MoE) language models are characterized by total and active parameters, e.g., Qwen3-235B-A22B (Yang et al., 2025) and OLMoE-1B-7B (Muennighoff et al., 2024). This is likely due to the following practical deployment considerations: Total parameters determine the model's memory footprint, while active parameters influence the computational cost during inference; both factors also fundamentally influence training latency.

Despite their prevalence, these two parameters are insufficient to fully characterize an MoE architecture. To resolve this ambiguity, we define an MoE architecture using five variables: Number of layers or depth (l), hidden dimension or width (d), number of experts (n_{exp}), number of activated experts (n_{topk}), and the ratio of hidden dimension to expert hidden dimension (granularity, $g := d/d_{exp}$). For a multi-head attention-based MoE model, the

non-embedding parameter counts are: ¹

$$N_{total} \approx ld^2 (4 + 3n_{exp}/g) \quad (1)$$

$$N_{active} \approx ld^2 (4 + 3n_{topk}/g) \quad (2)$$

Even if we constrain N_{total} and N_{active} , there are still multiple choices of width, depth, and MoE configuration that satisfy the above two constraints. This raises an important question: *Given upper bounds on memory and inference, how should one select the variables to optimize performance?*

In this paper, we conduct a systematic study to identify the optimal configuration within a fixed budget of N_{total} and N_{active} ($N_{total} > N_{active}$). We show that as long as the width-to-depth ratio and granularity are within reasonable ranges, performance is mainly determined by N_{total} and expert sparsity $s := n_{exp}/n_{topk}$. Furthermore, we identify a specific n_{exp} penalty. For a fixed sparsity ratio, increasing n_{exp} requires a compensatory reduction in the model's core dimensions (l and d) to stay within the total parameter budget. This reduction leads to a net decrease in the active compute capacity per token, which slightly penalizes performance. These findings allow us to derive a principle that determines the optimal MoE configuration that maximizes N_{total} while minimizing s (maximizing n_{topk}) and n_{exp} under the given constraints. By fitting scaling laws across models and dataset sizes, we also test and validate our principle on two representative architectures.

Related work. Various aspects of MoE models (Shazeer et al., 2017; Lepikhin et al.; Fedus et al., 2022) have been studied in the literature. For a comprehensive survey of MoE models, please refer to Cai et al. (2024). We here only review the most relevant ones, which often relate the loss/performance

¹For convenience, total and active parameters are always referred to as non-embedding parameters in this paper; a more precise description of configurations is given in Appendix A.

of MoE models to the model configuration via scaling laws.

Clark et al. (2022) are among the first to propose a scaling law for MoE models, showing that the loss is a function of N_{total} and n_{exp} . Krajewski et al. (2024); Liew et al. (2025); Abnar et al. (2025); Ludziejewski et al. (2025); Tian et al. (2025) study aspects such as granularity, upcycling, sparsity, memory efficiency and dense-to-MoE efficiency ratio. While conclusions differ among studies, the consensus is that total parameters and/or active parameters are the most important factors affecting the performance of MoE models. There is however no work trying to disentangle the interplay of all the parameters appearing in Equations 1 and 2 given total parameters and active parameters, as far as we know.

Setup. We use an architecture closely resembling that of Qwen3 (Yang et al., 2025), which in turn follows the architecture of (Fedus et al., 2022), scaling the feed-forward (FFN) layers of transformer-based language models into n_{exp} experts and activating only n_{topk} of them for each input token. Furthermore, the fine-grained MoE architecture is adopted with the FFN hidden dimension g times smaller than the attention hidden dimension (Dai et al., 2024; Krajewski et al., 2024).

The models are trained using a standard language modeling objective on the FineWeb-Edu dataset (Penedo et al., 2024), with its performance evaluated on a held-out dataset. More details about training hyperparameters and model configurations can be found in Appendix A.

2 Ablation fixing Total and Active Parameters

As discussed above, total and active parameters are vital at specifying MoE models. We first conduct ablation studies by fixing (approximately) these two parameters and varying other configurations to understand how different combinations of parameters change the loss.

2.1 Granularity

We study the effect of granularity g by varying n_{exp}, n_{topk} in conjunction with d_{exp} such that the total and active parameters are fixed. Higher g means finer granularity; i.e., smaller expert hidden dimension d_{exp} , but more experts.

Table 1 shows the results of this ablation study on two different model sizes. We see that g of 4

l	d	g	n_{exp}	n_{topk}	Loss diff (%)
8	384	2	64	4	0.7%
		4	128	8	0.48%
		8	256	16	0.00%
		16	512	32	0.21%
18	1024	2	64	4	1.04%
		4	128	8	0.00%
		8	256	16	0.29%
		16	512	32	0.58%

Table 1: Ablation study on granularity g with fixed total and active parameters. See Appendix B for more results.

l	d	d/l	n_{nexp}	n_{topk}	Loss diff (%)
16	240	15	43	4	0.65%
		8	336	42	43
		4	480	120	43
		16	160	10	103
8	224	28	103	16	1.12%
		4	320	80	103
		16	160	10	103
		4	224	28	103

Table 2: Ablation study on the width-to-depth ratio $\gamma = d/l$ with approximately the same total and active parameters. See Appendix B for more results.

to 8 generally minimize the loss, while increasing g leads to diminishing returns. Our results largely agree with Tian et al. (2025) that g (in our notations) between 4 and 6 is a good choice. We use $g = 4$ in the following experiments.

2.2 Width-to-depth Ratio

Next, we wish to study the choice of width-to-depth ratio $\gamma := d/l$. We vary all relevant parameters in Equations 1 and 2 while keeping total and active parameters fixed approximately (g is fixed to 4).

We see in Table 2 that models with the lowest γ (e.g., 10) generally have higher loss, while those with mid-range values (e.g., 42) achieve the lowest loss in configurations explored. However, simply increasing γ to the maximum (136) does not guarantee the lowest loss, suggesting a sweet spot. We consequently choose to follow the standard setting of Kaplan et al. (2020) by keeping γ between 32 and 64.

3 Scaling Laws for MoE Design

To systematically identify the optimal MoE architecture, we must navigate the five degrees of freedom ($l, d, n_{exp}, n_{topk}, g$) present in Equations 1 and 2. In the previous Section, we have constrained two of these dimensions to values that

minimize loss while maintaining fixed total and active parameter budgets, reducing the remaining degrees of freedom to three; there is still ambiguity in determining the configuration.

In this Section, we vary the variables (under aforementioned constraints) across a wide range of model scales (30M to 3B parameters; details in Appendix C), under a fixed training token budget, to study the loss behavior with respect to these variables, such that we can find the remaining (optimal) configuration that minimizes the loss.

We assume a power-law relationship between loss and the variables (Hestness et al., 2017, 2019), such that we can perform linear regression on the log-log scale (e.g., $\log L = \alpha \log N_{total} + \beta$). This allows us to perform statistically robust fitting and hypothesis testing on each variable’s significance.

3.1 Results

The loss values with respect to N_{total} are shown in Figure 1. We see that loss generally decreases with N_{total} as a power law. However, there is a large variance in loss values for similar N_{total} , suggesting that other factors are at play. Moreover, optimizing loss based on N_{total} alone cannot resolve for the optimal configuration.

We list the results of fitting various combinations of variables in Table 3. The performance of each function is mainly evaluated with the R^2 value of the fit, with additional scrutiny provided by t-tests for variable significance and condition numbers to detect collinearity.

Our analysis yields the following observations:

- **Dominance of total parameters.** N_{total} is a significantly stronger predictor of performance ($R^2 = 0.926$) than N_{active} ($R^2 = 0.641$) when used as a single baseline.
- **Total and active parameters.** While the interaction function $\log(N_{total}) + \log(N_{active}) + \log(N_{total})\log(N_{active})$ achieves the highest R^2 (0.988), it suffers from strong multicollinearity problem.
- **Sparsity’s role.** Adding s to either N_{total} or N_{active} significantly improves the fit, achieving R^2 values of 0.983 and 0.944 respectively. Still, adding s cannot resolve the ambiguity in MoE configuration because multiple combinations of (n_{exp}, n_{topk}) are still possible.
- **Disambiguated function.** We propose the use of $(N_{total}, n_{exp}, n_{topk})$ as the primary scaling

law. This model achieves an R^2 of 0.985 with all variables being statistically significant and it fully resolves the MoE configuration.

The resulting fitted scaling law is as follows:

$$L \propto N_{total}^{-0.052} n_{exp}^{0.023} n_{topk}^{-0.018} \quad (3)$$

$$= N_{total}^{-0.052} s^{0.018} n_{exp}^{0.005} \quad (4)$$

The fact that lower sparsity s leads to better performance aligns with the intuition that activating more experts allows for better utilization of model capacity. Furthermore, the n_{exp} penalty can be interpreted as follows: To maintain a fixed N_{total} , the core dimensions (l, d) must be reduced to compensate for the larger n_{exp} . Because N_{active} is scaled by these same dimensions, the net result is a decrease in active parameters per token, leading to a performance penalty due to reduced compute capacity. See Appendix C.2 for a more precise mathematical justification.

Our results imply the following principle for optimal configuration: Maximize N_{total} , n_{topk} and minimize n_{exp} to minimize the loss according to Equation 4 while satisfying constraints on g , γ , and N_{active} , leaving no ambiguity in the configuration.

Note however practical design is further constrained by the fact that the parameters in Equations 1 and 2 must be integers. Additionally, d must satisfy divisibility constraints due to attention head partitioning and parallelism (when tensor parallelism is used) requirements. Consequently, we propose the following iterative routine: First, we maximize N_{total} by solving for the largest (l, d) within memory, g and partitioning constraints, looping over γ, n_{exp} . Second, we maximize n_{topk} until the inference budget is saturated. This routine ensures maximum leverage of available memory while preventing performance penalty incurred by excessive n_{exp} . We give a more detailed discussion in Appendix C.3.

3.2 Testing the Design Principle by comparing two Configurations

The scaling law in Equation 4 is based on models trained with a fixed token budget. To test its effectiveness in guiding MoE design, we conduct experiments by training models under various model and dataset sizes, fixing two configurations due to computational resource constraints. Specifically, we compare MoE configurations with the same s : $(n_{exp}, n_{topk}) = (128, 8), (256, 16)$. We

Variables	R^2	Result/Intrepretation
<i>Simple Baseline</i>		
$\log(N_{total})$ only	0.926	Baseline (Total params).
$\log(N_{active})$ only	0.641	Baseline (Active params).
<i>Core Functions</i>		
$\log(N_{active}) + \log(s)$	0.944	Moderately good fit.
$\log(N_{total}) + \log(s)$	0.983	Good fit.
$\log(N_{total}) + \log(n_{exp}) + \log(n_{topk})$	0.985	Good and disambiguated fit.
$\log(N_{active}) + \log(n_{exp}) + \log(n_{topk})$	0.981	Moderately good fit.
<i>Interaction Functions</i>		
$\log(N_{total}) + \log(s) + \log(N_{total}) \log(s)$	0.983	Interaction term redundant.
$\log(N_{total}) + \log(N_{active}) + \log(N_{total}) \log(N_{active})$	0.988	Strong multicollinearity problem.
<i>Other Combinations</i>		
$\log(N_{total}) + \log(N_{active}) + \log(s)$	0.985	N_{active} 's significance is low.

Table 3: Results of fitting various combinations of variables to loss. More results in Table 8 of Appendix C.

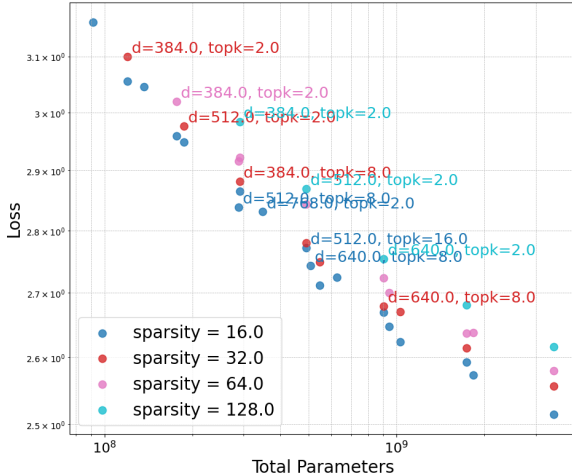


Figure 1: Loss vs. Total Parameters. Each point represents a model with a specific configuration.

fit Chinchilla-style scaling laws (Hoffmann et al., 2022) for these configurations:

$$L_{128/8 \text{ or } 256/16} = AN_{total}^{-\alpha} + BD^{-\beta} + E \quad (5)$$

where D is the dataset size (in tokens) and A, B, E, α, β are fitted coefficients. According to Equation 4, the (128, 8) configuration should outperform the (256, 16) one, when compared under the same N_{total} , s , and D , as it has smaller n_{exp} .

We perform experiments and fit the scaling laws accordingly (see Appendix C for details). The resulting curves are shown in Figure 2. Indeed, the (128, 8) configuration consistently outperforms the (256, 16) one under the same N_{total} and D , confirming the effectiveness of our design principle.

We note that previous works (Abnar et al., 2025; Tian et al., 2025) have attempted to fit scaling

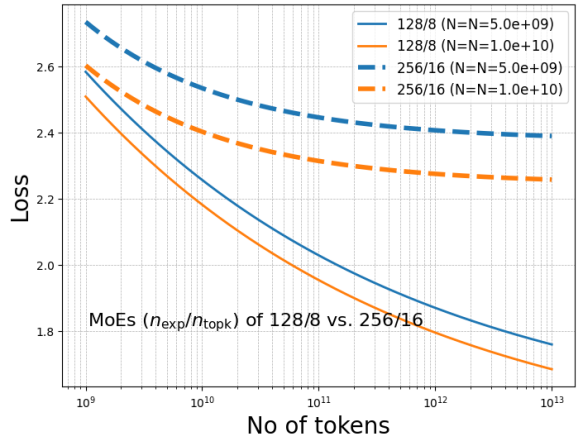


Figure 2: Comparison of loss between the (128, 8) and (256, 16) configurations with fitted scaling laws.

laws involving model configuration and dataset size. However, they studied only s without disentangling n_{exp} and n_{topk} . Our results indicate that a more complete scaling law involving all these factors would be desirable.

4 Conclusion

MoE models are mainstream for large language models (Jiang et al., 2024; Dai et al., 2024; Yang et al., 2025), yet their optimal configuration has remained poorly understood. We disentangle the MoE configuration to show that N_{total} is the primary predictor of performance, followed by expert sparsity s and total experts n_{exp} . Our design principle of optimizing these quantities under other conditions provides a rigorous foundation for building more efficient MoE models under practical constraints.

Limitations

The first significant limitation is the scale of our experiments. Due to limited computational resources, we are only able to conduct experiments on small to medium-sized models and datasets, with limited architecture search (we perform a kind of greedy search by first determining the optimal values of g and γ before moving on to deriving the scaling law) and hyperparameter tuning. While we believe that our findings provide valuable insights into the design of MoE models, further validation on a larger scale, and more refined search/tuning is necessary to confirm their generalizability. Ultimately, a full scaling law involving model configuration and dataset size would be desirable (which would require full grid search over model configuration, model size and dataset size).

The second limitation pertains to our use of total parameters and active parameters as proxies for memory and inference/training costs, respectively. While these proxies are commonly used in the literature, they may not fully capture the complexities of real-world deployment scenarios. Factors such as hardware architecture, software optimizations, parallelism training techniques, and specific use cases can significantly influence the actual memory footprint and inference latency of MoE models.

Acknowledgements

We would like to thank Takuya Kato for helpful discussions and feedback.

References

Samira Abnar, Harshay Shah, Dan Busbridge, Alaaeldin Mohamed Elnouby Ali, Josh Susskind, and Vimal Thilak. 2025. Parameters vs flops: Scaling laws for optimal sparsity for mixture-of-experts language models. *arXiv preprint arXiv:2501.12370*.

Tamay Besiroglu, Ege Erdil, Matthew Barnett, and Josh You. 2024. Chinchilla scaling: A replication attempt. *arXiv preprint arXiv:2404.10102*.

Weilin Cai, Juyong Jiang, Fan Wang, Jing Tang, Sunghun Kim, and Jiayi Huang. 2024. A survey on mixture of experts. *arXiv preprint arXiv:2407.06204*.

Aidan Clark, Diego de Las Casas, Aurelia Guy, Arthur Mensch, Michela Paganini, Jordan Hoffmann, Bogdan Damoc, Blake Hechtman, Trevor Cai, Sebastian Borgeaud, and 1 others. 2022. Unified scaling laws for routed language models. pages 4057–4086. PMLR.

Damai Dai, Chengqi Deng, Chenggang Zhao, RX Xu, Huazuo Gao, Deli Chen, Jiashi Li, Wangding Zeng, Xingkai Yu, Y Wu, and 1 others. 2024. Deepseekmoe: Towards ultimate expert specialization in mixture-of-experts language models. *arXiv preprint arXiv:2401.06066*.

Tri Dao, Dan Fu, Stefano Ermon, Atri Rudra, and Christopher Ré. 2022. Flashattention: Fast and memory-efficient exact attention with io-awareness. *Advances in Neural Information Processing Systems*, 35:16344–16359.

William Fedus, Barret Zoph, and Noam Shazeer. 2022. Switch transformers: Scaling to trillion parameter models with simple and efficient sparsity. *Journal of Machine Learning Research*, 23(120):1–39.

Alex Hägele, Elie Bakouch, Atli Kosson, Leandro Von Werra, Martin Jaggi, and 1 others. 2024. Scaling laws and compute-optimal training beyond fixed training durations. *Advances in Neural Information Processing Systems*, 37:76232–76264.

Alex Henry, Prudhvi Raj Dachapally, Shubham Shantaram Pawar, and Yuxuan Chen. 2020. Query-key normalization for transformers. In *Findings of the Association for Computational Linguistics: EMNLP 2020*, pages 4246–4253.

Joel Hestness, Newsha Ardalani, and Gregory Diamos. 2019. Beyond human-level accuracy: Computational challenges in deep learning. pages 1–14.

Joel Hestness, Sharan Narang, Newsha Ardalani, Gregory Diamos, Heewoo Jun, Hassan Kianinejad, Md Mostofa Ali Patwary, Yang Yang, and Yanqi Zhou. 2017. Deep learning scaling is predictable, empirically. *arXiv preprint arXiv:1712.00409*.

Jordan Hoffmann, Sebastian Borgeaud, Arthur Mensch, Elena Buchatskaya, Trevor Cai, Eliza Rutherford, Diego de Las Casas, Lisa Anne Hendricks, Johannes Welbl, Aidan Clark, and 1 others. 2022. Training compute-optimal large language models. *Proceedings of the 36th International Conference on Neural Information Processing Systems*, pages 30016–30030.

Albert Q Jiang, Alexandre Sablayrolles, Antoine Roux, Arthur Mensch, Blanche Savary, Chris Bamford, Devendra Singh Chaplot, Diego de las Casas, Emma Bou Hanna, Florian Bressand, and 1 others. 2024. Mixtral of experts. *arXiv preprint arXiv:2401.04088*.

Jared Kaplan, Sam McCandlish, Tom Henighan, Tom B Brown, Benjamin Chess, Rewon Child, Scott Gray, Alec Radford, Jeffrey Wu, and Dario Amodei. 2020. Scaling laws for neural language models. *arXiv preprint arXiv:2001.08361*.

Jakub Krajewski, Jan Ludziejewski, Kamil Adamczewski, Maciej Pióro, Michał Krutul, Szymon Antoniak, Kamil Ciebiera, Krystian Król, Tomasz Odrzygóźdż, Piotr Sankowski, and 1 others. 2024.

Scaling laws for fine-grained mixture of experts. *arXiv preprint arXiv:2402.07871*.

Dmitry Lepikhin, HyoukJoong Lee, Yuanzhong Xu, Dehao Chen, Orhan Firat, Yanping Huang, Maxim Krikun, Noam Shazeer, and Zhipeng Chen. Gshard: Scaling giant models with conditional computation and automatic sharding.

Margaret Li, Sneha Kudugunta, and Luke Zettlemoyer. 2025. (mis) fitting: A survey of scaling laws. *arXiv preprint arXiv:2502.18969*.

Seng Pei Liew, Takuya Kato, and Sho Takase. 2025. **Scaling laws for upcycling mixture-of-experts language models.** In *Proceedings of the 42nd International Conference on Machine Learning*, volume 267 of *Proceedings of Machine Learning Research*, pages 37682–37704. PMLR.

Ilya Loshchilov, Frank Hutter, and 1 others. 2017. Fixing weight decay regularization in adam. *arXiv preprint arXiv:1711.05101*, 5.

Jan Ludziejewski, Maciej Pióro, Jakub Krajewski, Maciej Stefański, Michał Krutul, Jan Małański, Marek Cygan, Piotr Sankowski, Kamil Adamczewski, Piotr Miłoś, and 1 others. 2025. Joint moe scaling laws: Mixture of experts can be memory efficient. *arXiv preprint arXiv:2502.05172*.

Niklas Muennighoff, Luca Soldaini, Dirk Groeneveld, Kyle Lo, Jacob Morrison, Sewon Min, Weijia Shi, Pete Walsh, Oyvind Tafjord, Nathan Lambert, and 1 others. 2024. Olmoe: Open mixture-of-experts language models. *arXiv preprint arXiv:2409.02060*.

Guilherme Penedo, Hynek Kydliček, Anton Lozhkov, Margaret Mitchell, Colin A Raffel, Leandro Von Werra, Thomas Wolf, and 1 others. 2024. The fineweb datasets: Decanting the web for the finest text data at scale. *Advances in Neural Information Processing Systems*, 37:30811–30849.

Tomer Porian, Mitchell Wortsman, Jenia Jitsev, Ludwig Schmidt, and Yair Carmon. 2024. Resolving discrepancies in compute-optimal scaling of language models. *Advances in Neural Information Processing Systems*, 37:100535–100570.

Skipper Seabold and Josef Perktold. 2010. statsmodels: Econometric and statistical modeling with python. In *9th Python in Science Conference*.

Noam Shazeer, Azalia Mirhoseini, Krzysztof Maziarz, Andy Davis, Quoc Le, Geoffrey Hinton, and Jeff Dean. 2017. Outrageously large neural networks: The sparsely-gated mixture-of-experts layer.

Mohammad Shoeybi, Mostofa Patwary, Raul Puri, Patrick LeGresley, Jared Casper, and Bryan Catanzaro. 2019. Megatron-lm: Training multi-billion parameter language models using model parallelism. *arXiv preprint arXiv:1909.08053*.

Jianlin Su, Murtadha Ahmed, Yu Lu, Shengfeng Pan, Wen Bo, and Yunfeng Liu. 2024. Roformer: Enhanced transformer with rotary position embedding. *Neurocomputing*, 568:127063.

Changxin Tian, Kunlong Chen, Jia Liu, Ziqi Liu, Zhiqiang Zhang, and Jun Zhou. 2025. Towards greater leverage: Scaling laws for efficient mixture-of-experts language models. *arXiv preprint arXiv:2507.17702*.

Ashish Vaswani, Noam Shazeer, Niki Parmar, Jakob Uszkoreit, Llion Jones, Aidan N Gomez, Łukasz Kaiser, and Illia Polosukhin. 2017. Attention is all you need. *Advances in neural information processing systems*, 30.

An Yang, Anfeng Li, Baosong Yang, Beichen Zhang, Bin Yuan Hui, Bo Zheng, Bowen Yu, Chang Gao, Chengen Huang, Chenxu Lv, and 1 others. 2025. Qwen3 technical report. *arXiv preprint arXiv:2505.09388*.

A More on Our Setup

A.1 Model Setup

As described in the main text, we use a Qwen3-like MoE architecture (Yang et al., 2025), adopting advances such as QK-norm (Henry et al., 2020), Rope positional encoding (Su et al., 2024) beyond the original transformer architecture (Vaswani et al., 2017). Our tokenizer is the same as that of Qwen3.

We do not use grouped-query attention in our experiments, as it introduces an additional hyperparameter (the number of query groups) that complicates the analysis. We also do not consider shared experts (Dai et al., 2024) in this work.

The parameters we vary are listed below:

- Number of layers l
- Hidden dimension d
- MoE hidden dimension d_{exp} or granularity g
- Number of experts n_{exp}
- Number of activated experts n_{topk}

We fix the attention head number to 4 for all models (Porian et al., 2024). The main model configurations used in Section 3 is summarized in Table 4 (g fixed to 4).

A.2 Experimental Setup

Here, we give a more detailed description of the experimental setup. Our experiments are conducted using the Megatron-LM framework (Shoeybi et al., 2019). Models are trained with mixed precision.

l	d	N_{total} for (128,8)
6	288	49,766,400
6	384	88,473,600
8	384	117,964,800
8	512	209,715,200
10	640	409,600,000
14	768	825,753,600
16	1024	1,677,721,600

Table 4: Model configuration used in experiments in Section 3. N_{total} is calculated with $g = 4, n_{exp} = 128, n_{topk} = 8$.

We also use optimization libraries like FlashAttention (Dao et al., 2022) and TransformerEngine².

We adopt the WSD learning rate schedule for all experiments. In the final phase of training, the learning rate decays linearly to 10% of its peak value, with the decay phase spanning roughly 10% of the total training steps, following the setup in Hägele et al. (2024). To emulate varying token budgets, we save intermediate checkpoints and perform continued learning on them with decayed learning rates. We set warmup iterations, batch size and learning rate as 100, 2048 and 10^{-3} respectively for most of the experiments unless stated otherwise. This leads to more stable fitting (Li et al., 2025). Additional configurations are as in Table 5.

B More on Ablation Studies

Granularity. Table 6 additionally shows the loss difference in percentage compared to the best configuration in Table 1. We further note that the uncertainty in loss values due to random seeds is around 0.4%. The smaller model ($l = 8, d = 384$) is trained with 9B tokens. For the larger model ($l = 18, d = 1024$), we increase the training tokens and warmup steps to 46B and 500 respectively.

Width-to-depth ratio. Table 7 shows more results of the width-to-depth ratio ablation study and in more detail, where we additionally show the percentage difference in total and active parameters compared to the best configuration in Table 2 (because we cannot obtain the exact values while varying model architecture). We further note that the uncertainty in loss values due to random seeds is around 0.8%. Models are trained for 4B tokens.

C More on Scaling Laws

C.1 MoE Design

Here, we give more details about the experiments conducted in Figure 1 in Section 3. The (n_{exp}, n_{topk}) configurations used are (32,2), (64,2), (64,4), (128,2), (128,8), (256,2), (256,4), (256,8), and (256,16), combined with the core dimensions in Table 4. All models are trained for 9B tokens.

For fitting the scaling laws, we take the logarithm of all variables and perform linear regression using the ordinary least squares (OLS) method. We use the `statsmodels` library for fitting and statistical tests (Seabold and Perktold, 2010). The test of significance for each variable is performed using t-tests, with a significance level of 0.05.

We show more combinations of variables tried in Table 3 in Table 8, particularly repeating the same combinations from Table 3 but including more combinations involving N_{active} . We see that some combinations, e.g., $(N_{total}, N_{active}, n_{exp})$ and $(N_{total}, N_{active}, n_{topk})$ are also quite effective (although slightly smaller R^2). However, our choice of $(N_{total}, n_{exp}, n_{topk})$ is more interpretable, as it is connected to sparsity s directly (of which the component variables are easy to configure), additionally allowing the mathematical interpretation of the n_{exp} penalty as described in the main text.

We further visualize the goodness of fit for the selected scaling law in Figure 3.

C.2 Derivation of the n_{exp} Penalty under Fixed Constraints

To understand why increasing the number of experts n_{exp} penalizes performance when total parameters N_{total} and expert sparsity s are fixed, we examine the relationship between active parameters N_{active} and n_{exp} .

We start from parameter countings, reiterating the equations for total and active parameters:

$$N_{total} \approx ld^2 \left(4 + \frac{3n_{exp}}{g} \right)$$

$$N_{active} \approx ld^2 \left(4 + \frac{3n_{topk}}{g} \right)$$

Given that expert sparsity is defined as $s = n_{exp}/n_{topk}$, we substitute $n_{topk} = n_{exp}/s$. To isolate the effect of n_{exp} while holding N_{total} constant, we first solve for the core dense term ld^2 :

$$ld^2 \approx \frac{N_{total}}{4 + \frac{3n_{exp}}{g}}$$

²<https://github.com/NVIDIA/TransformerEngine>

Configuration	Value
Context length	2048
Embedding	Tied
Optimizer	AdamW (Loshchilov et al., 2017)
Adam β_1	0.9
Adam β_2	0.95
Weight decay	0.1
Gradient clipping	1.0
MoE load balancing loss coefficient	10^{-3}

Table 5: Training configurations.

l	d	$g (d/d_{moe})$	n_{exp}	n_{topk}	Loss	Loss diff (%)
8	384	1	32	2	2.995	1.7%
8	384	2	64	4	2.966	0.7%
8	384	4	128	8	2.960	0.48%
8	384	8	256	16	2.945	0.00%
8	384	16	512	32	2.951	0.21%
18	1024	1	32	2	2.334	1.64%
18	1024	2	64	4	2.320	1.04%
18	1024	4	128	8	2.297	0.00%
18	1024	8	256	16	2.304	0.29%
18	1024	16	512	32	2.310	0.58%

Table 6: Detailed results for the granularity g ablation study with fixed total and active parameters.

Substituting this back into the equation for N_{active} :

$$N_{active} \approx \left(\frac{N_{total}}{4 + \frac{3n_{exp}}{g}} \right) \cdot \left(4 + \frac{3n_{exp}}{gs} \right)$$

The ratio of active to total parameters is thus:

$$\frac{N_{active}}{N_{total}} \approx \frac{4 + \frac{3n_{exp}}{gs}}{4 + \frac{3n_{exp}}{g}}$$

In the standard MoE regime where $s > 1$, the denominator grows faster than the numerator as n_{exp} increases. Consequently, N_{active} must decrease to satisfy the constant N_{total} constraint. This confirms that for a fixed memory budget, a larger total number of experts mathematically necessitates a reduction in the model’s active compute, leading to the observed performance penalty.

C.3 Architectural Optimization Routine

To determine the optimal configuration $(l, d, n_{exp}, n_{topk})$, we treat the expert count n_{exp} and the width-to-depth ratio $\gamma = d/l$ as hyperparameters. For each combination, we solve for the maximum dimensions allowed by the memory and inference constraints, denoted by

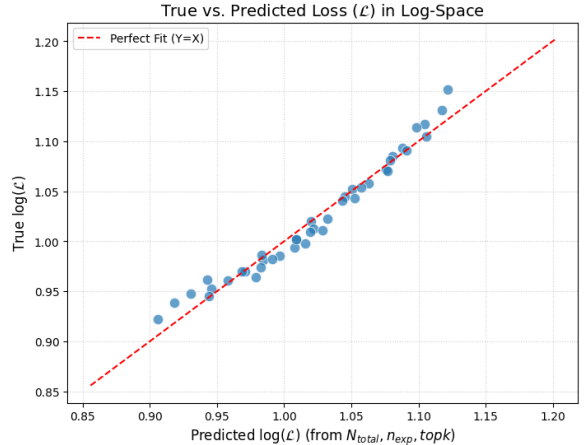


Figure 3: Goodness of fit for the selected scaling law in Section 3.

l	d	$\gamma(d/l)$	n_{nexp}	n_{topk}	Loss	Loss diff (%)	N_{active} diff (%)	N_{total} diff (%)
16	272	17	32	2	3.19	0.19%	2.98%	1.24%
8	384	48	32	2	3.21	0.84%	2.62%	0.89%
4	544	136	32	2	3.20	0.50%	2.98%	1.24%
16	240	15	43	4	3.21	0.65%	2.04%	2.04%
8	336	42	43	4	3.19	0.00%	0.00%	0.00%
4	480	120	43	4	3.22	1.12%	2.04%	2.04%
16	160	10	103	16	3.27	2.68%	3.66%	1.65%
8	224	28	103	16	3.26	2.20%	1.59%	-0.38%
4	320	80	103	16	3.24	1.68%	3.66%	1.65%

Table 7: Detailed results for the width-to-depth ratio d/l ablation study with approximately fixed total and active parameters. g is fixed to 4.

Variables	R^2	Result/Intrepretation
<i>Simple Baseline</i>		
$\log(N_{total})$ only	0.926	Baseline (Total params).
$\log(N_{active})$ only	0.641	Baseline (Active params).
<i>Core Functions</i>		
$\log(N_{active}) + \log(s)$	0.944	Moderately good fit.
$\log(N_{total}) + \log(s)$	0.983	Good fit.
$\log(N_{total}) + \log(n_{exp}) + \log(n_{topk})$	0.985	Good and disambiguated fit.
$\log(N_{active}) + \log(n_{exp}) + \log(n_{topk})$	0.981	Moderately good fit.
<i>Interaction Functions</i>		
$\log(N_{total}) + \log(s) + \log(N_{total}) \log(s)$	0.983	Interaction term redundant.
$\log(N_{total}) + \log(N_{active}) + \log(N_{total}) \log(N_{active})$	0.988	Strong multicollinearity problem.
<i>Other Combinations</i>		
$\log(N_{total}) + \log(N_{active}) + \log(s)$	0.985	N_{active} ’s significance is low.
$\log(N_{total}) + \log(N_{active})$	0.979	Moderately good fit.
$\log(N_{total}) + \log(N_{active}) + \log(n_{exp})$	0.983	Good fit.
$\log(N_{total}) + \log(N_{active}) + \log(n_{topk})$	0.984	Good fit.

Table 8: Results of fitting various combinations of variables to the loss values.

C_{total} and C_{active} . The pseudocode is given in Algorithm 1. In plain language, for each n_{exp} and γ , we first solve for the maximum l satisfying the total capacity constraint. Then, we solve for the maximum d satisfying the same constraint while ensuring that d is aligned to k_{align} (to account for attention head partitioning or hardware alignment requirements). Finally, we solve for the maximum n_{topk} satisfying the inference constraint.

The scaling law $L \propto N_{total}^{-0.052} n_{exp}^{0.023} n_{topk}^{-0.018}$ reveals a critical trade-off. While increasing n_{exp} allows for a larger N_{total} within a fixed memory budget, the positive exponent (0.023) acts as a penalty. The optimization loop ensures that the gain from N_{total} outweighs this penalty, while n_{topk} is used as the final lever to recover performance within the inference constraint.

Comparison with Qwen3-235B-A22B. Using the optimization routine, we derive an MoE configuration under similar memory and inference constraints as Qwen3-235B-A22B. Using the Qwen3 memory and inference constraints, our optimization routine suggests an MoE configuration of $(l, d, n_{exp}, n_{topk}) = (94, 4096, 128, 7)$, resulting in 234B total parameters and 21.7B active parameters. This configuration is close to that of Qwen3-235B-A22B but with more layers, which uses $(l, d, n_{exp}, n_{topk}) = (83, 5312, 128, 8)$. We also note that Qwen3-235B-A22B uses $g = 2.7$.

C.4 Testing the MoE Design Principle

We describe the settings for the experiments in Figure 2 in Section 3. The models (configurations in Table 4) are trained with various dataset sizes (from 9B to 50B tokens).

Algorithm 1 MoE Architectural Optimization

```

1: Input: Memory constraint  $C_{total}$ , Inference
   constraint  $C_{active}$ , Alignment factor  $k_{align}$ 
2: Parameters:  $\Gamma \in [32, 64]$ ,  $n_{exp} \in$ 
    $\{2^1, 2^2, \dots, 2^k\}$ 
3: Initialize:  $L_{min} \leftarrow \infty, \theta^* \leftarrow \emptyset$ 
4: for each  $n_{exp} \in \{2^1, \dots, 2^k\}$  do
5:   for each  $\gamma \in \Gamma$  do
6:      $l \leftarrow \lfloor (C_{total}/(\gamma^2(4 + 0.75n_{exp})))^{1/3} \rfloor$ 
7:      $d \leftarrow \text{round}(\gamma \cdot l/k_{align}) \cdot k_{align}$ 
8:     while  $l \cdot d^2 \cdot (4 + 0.75n_{exp}) > C_{total}$  do
9:        $d \leftarrow d - k_{align}$ 
10:      end while
11:       $n_{topk} \leftarrow \min \left( n_{exp}, \lfloor \frac{4}{3} \left( \frac{C_{active}}{ld^2} - 4 \right) \rfloor \right)$ 
12:      if  $n_{topk} \geq 1$  then
13:         $L \leftarrow (ld^2(4 + 0.75n_{exp}))^{-0.052} \cdot$ 
            $n_{exp}^{0.023} \cdot n_{topk}^{-0.018}$ 
14:        if  $L < L_{min}$  then
15:           $L_{min} \leftarrow L, \theta^* \leftarrow (l, d, n_{exp}, n_{topk})$ 
16:        end if
17:      end if
18:    end for
19:  end for
20: return  $\theta^*$ 

```

We fit the losses with the functional form of Chinchilla-style scaling laws following (Hoffmann et al., 2022; Besiroglu et al., 2024): We perform optimization using the Huber loss ($\delta = 10^{-3}$) and the BFGS algorithm, to fit the logarithm of the loss via the LogSumExp trick applied to the RHS of functional forms. The fitted coefficients are as follows:

- For the (128,8) configuration: $A = 28, B = 229, E = 1.08, \alpha = 0.28, \beta = 0.16$
- For the (256,16) configuration: $A = 564, B = 640,500, E = 2.0, \alpha = 0.64, \beta = 0.36$

We further visualize the goodness of fit in Figure 4 and 5.

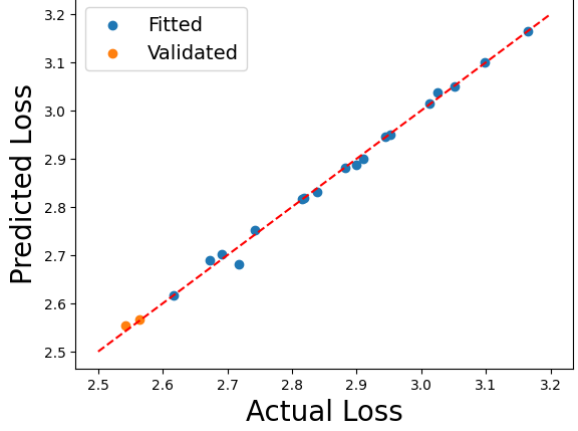


Figure 4: Goodness of fit for the (128,8) configuration.

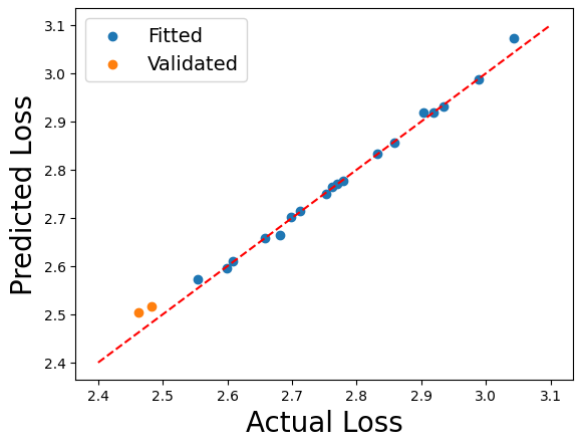


Figure 5: Goodness of fit for the (256,16) configuration.